American Physiological Society | Journal of Neurophysiology

PUBLISHED ARTICLE
ARCHIVES
SUBSCRIPTIONS
SUBMISSIONS
CONTACT US

J Neurophysiol. 2011 Oct; 106(4): 1923–1932.
Published online 2011 Jul 13. doi: 10.1152/jn.00095.2011

PMCID: PMC3191844

Development of cortical orientation selectivity in the absence of visual experience with contour

Tomokazu Ohshiro,[*] Shaista Hussain, and Michael Weliky

Department of Brain and Cognitive Sciences, Center for Visual Science, University of Rochester, Rochester, New York

[*]Corresponding author.

Address for reprint requests and other correspondence: T. Ohshiro, Dept. of Brain and Cognitive Sciences, Center for Visual Science, Meliora Hall, Univ. of Rochester, Rochester, NY 14627 (e-mail: toshiro@bcs.rochester.edu).

Received 2011 Feb 2; Accepted 2011 Jul 11.

Abstract

Visual cortical neurons are selective for the orientation of lines, and the full development of this selectivity requires natural visual experience after eye opening. Here we examined whether this selectivity develops without seeing lines and contours. Juvenile ferrets were reared in a dark room and visually trained by being shown a movie of flickering, sparse spots. We found that despite the lack of contour visual experience, the cortical neurons of these ferrets developed strong orientation selectivity and exhibited simple-cell receptive fields. This finding suggests that overt contour visual experience is unnecessary for the maturation of orientation selectivity and is inconsistent with the computational models that crucially require the visual inputs of lines and contours for the development of orientation selectivity. We propose that a correlation-based model supplemented with a constraint on synaptic strength dynamics is able to account for our experimental result.

Keywords: simple-cell receptive field, Hebbian learning rule, self-organization

NEURONS IN THE MATURE primary visual cortex are selective for the orientation of lines and edges (Hubel and Wiesel 1959). The selectivity is attributable to the simple-cell receptive field (RF), which is produced by the ordered projection of the ON-/OFF-center lateral geniculate nucleus (LGN) afferents onto cortical neurons (Hubel and Wiesel 1962; Reid and Alonso 1995; Tanaka 1983). Neurons with rudimentary orientation selectivity are present in the visually inexperienced cortex (Hubel and Wiesel 1963; Sherk and Stryker 1976); however, full maturation of this selectivity requires natural visual experience (Braastad and Heggelund 1985; Chapman et al. 1996; Crair et al. 1998; White et al. 2001). Because of the strong effect of oriented visual stimuli on the selectivity development (Blakemore and Cooper 1970; Blakemore and Van Sluyters 1975; Hirsch and Spinelli 1970, 1971; Stryker et al. 1978; Tanaka et al. 2006) and the abundance of oriented lines and contours in natural scenes, one may naturally assume that the visual experience of lines and contours during early life is essential for the development of orientation-selective responses in the visual cortex. Indeed, a number of neural network models have proposed that the simple-cell RF emerges as the result of the network's learning of lines and contours from visual inputs (Bell and Sejnowski 1997; Blais et al. 1998; Law and Cooper 1994; Olshausen and Field 1996; van Hateren and Ruderman 1998). However, rigorous experimental evidence supporting this idea seems to be lacking.

In this study, we raised juvenile ferrets in an artificial visual environment to examine whether orientation selectivity develops in the absence of contour visual experience. The rudimentary orientation selectivity in the developing cortex eventually dies out in the absence of any external visual input (Crair et al. 1998; White et al. 2001). Thus we had the juvenile ferrets view a movie of dynamically flickering, dark/bright, small spots that actively deprived them of contour visual experience. We found that the cortical neurons of these ferrets developed strong orientation selectivity and exhibited simple-cell RFs, suggesting that overt contour visual experience is not necessary for the continued maturation of orientation selectivity. The network models noted above cannot account for this experimental result. However, we show that a model with a simple correlation-based rule (Miller 1994) and a split constraint mechanism (Ohshiro and Weliky 2006) can account for our experimental result.

METHODS

All experimental procedures were approved by the University of Rochester Committee on Animal Resources. Male sable ferrets (Marshall Farms) were used in the experiments.

Visual training. The dark rearing of the ferret pups was started at the age of postnatal day (PND)26–28, ~1 wk before natural eye opening. Acclimation of these pups to the custom-made restraint chamber started immediately after the onset of the dark rearing. Custom-made restraint vests were used to restrain the ferrets in the chambers for up to 60 min per day in complete darkness. The trainer wore binocular night vision goggles (Rigel 3200 Pro, Rigel Optics) and conducted the pretraining acclimation sessions in complete darkness. Once their eyes were naturally open (around PND33–35), the visual training was started. The visual stimuli (movie) was projected on a large tangent screen (183 cm × 244 cm, dual vision; Delite system) spanning 112 × 126° of visual angle (Fig. 1*A*). An LCD projector (1,024 × 768 pixels, 60-Hz refresh rate; PowerLite 750c, Epson) was used to back-project the stimulus on the screen. The drifting-bar movie (Fig. 1*B*, *left*) showed high-contrast, full-field, black or white bars (width: 3° of visual angle) drifting in random directions at 11°/s on a gray background (luminescence 90 cd/m^2). The flickering-spots movie (Fig. 1*B*, *middle*) showed high-contrast black or white spots (diameter: 2.5°) appearing at random positions every 375 ms. The density of the spots was so low (1.1 per 10° × 10° area) that the probability of three or four spots joining to create an elongated contour was quite low. Assuming that the diameter of the RF of a cortical neuron, which typically ranges from 5° to 10° in adult ferrets (Chapman et al. 1991; Fiser et al. 2004; Smyth et al. 2003; Usrey et al. 2003), is 10° in young ferrets, an immature cortical neuron would "experience" such a contour for a short period (375 ms), as infrequently as once per ~12 min (see Supplemental Fig. S1).[1] To our knowledge, there is no literature reporting the cortical RF size of the juvenile ferrets. However, the RF center diameter of the immature LGN neurons ranges from 5° to 15° (Tavazoie and Reid 2000). Therefore, the RF size of the immature cortical neurons is reasonably estimated close to or larger than 10°. The drifting-spots movie (Fig. 1*B*, *right*) showed the same high-contrast black/white spots drifting continuously in random directions at 3.5°/s. The movies were rendered with Psychophysics Toolbox (Brainard 1997; Pelli 1997) supplemented by SimpleGL functions (Benjamin Singer, Princeton University). The distance between the screen and the animal was 60 cm. As the pups' necks and heads were snugly restrained with a soft cushion in the chamber, the pups could not rotate their heads or look around. Visual training was conducted for 30 min on the first day, and the training duration was gradually increased to a total of 4 h a day by the fourth week of training. The visual training was interrupted every 30–60 min for a break. The ferret pups were released from the chamber in complete darkness and returned to their mother in the cage during the break and after the training session. The visual training was continued until the animal was terminally examined between the fourth and seventh weeks of visual training (PND60–78). The total duration of visual training was between 41 and 73 h. One extra ferret pup was always included in each experimental group as a weight control. This animal did not take part in the visual training and remained with the mother in the dark room. Three of these weight-control ferrets were examined as dark-reared controls. The natural vision control ferrets were raised in the regular laboratory environment without any restraint under a 12:12-h day-night cycle. The restraint control ferrets

were exposed to the ordinary laboratory scenes while they were restrained in the restraint chamber. To provide them with richer visual experience, freely moving ferrets were placed in a transparent box (60 × 60 × 60 cm) in front of the restraint-conditioned ferrets during the training. After the visual training, they were returned to the cage in a dark room, as were the other movie-trained ferrets.

During the pilot and training experiments, we frequently monitored the animals' eyes to determine whether their eyes were gazing at the screen edges and how long their eyelids were physically open. The examiner stood near the side of the movie screen (~1.3 m away from the animal) and quickly checked the light reflection from each animal's retina with an ophthalmoscope; a faint beam of diffuse light was shown for a few seconds. We typically observed a light reflection from a tiny portion of the nasal retina but never observed animals at any age gazing at the examiner standing near the screen edges. Therefore, it is unlikely that animals saw the screen edges for a substantial time during visual training.

We consistently observed that animals younger than PND45 tended to close their eyes and struggle or fall asleep in the restraint chamber during the visual training. Their eyes were open for only 60% of the duration of stimulus presentation (19.5 ± 3.0 min per a 30-min-long training session; $n = 7$ animals at PND35–36, observed over 10 sessions). The older ferrets gazed at the screen calmly and were awake longer; their eyes were open for >80% of the duration of stimulus presentation (51.9 ± 1.6 min per a 1-h visual training session; $n = 8$ animals at PND57, observed over 7 sessions). When the ferret pup persisted in sleeping during the training, the trainer gently rubbed the pup's back or took the pup from the chamber and wrapped its body with his/her hands to awaken it. The trainer was extremely careful not to block the pup's visual field during the training.

Animal surgery and electrophysiology. Surgical anesthesia was induced with an intramuscular injection of ketamine hydrochloride (20 mg/kg) and xylazine (0.2 mg/kg). Banamine (0.5–2 mg/kg sc or im) and atropine sulfate (40–50 μg/kg im) were given after the induction of anesthesia. Intubation was performed, and the cephalic vein was cannulated for intravenous fluid infusion. Anesthesia was maintained with 1.5% isoflurane in pure oxygen. All surgical or pressured points were infiltrated with 0.25% bupivacaine. Heart rate, EEG, expired CO_2, and body temperature of the animal were monitored throughout the duration of the experiment. A small craniotomy and duratomy were made above the primary visual cortex for cortical recording. Low-melting, purified agarose (2.4%) was layered over the exposed cortex to prevent pulsation. After all surgical procedures were completed, animals were paralyzed with vecronium bromide (0.2 $mg \cdot kg^{-1} \cdot h^{-1}$ iv) and ventilated mechanically. The proper level of anesthesia was maintained by adjusting the isoflurane concentration (0.8–2%) and monitoring the EEG throughout the experiment. The accommodation reflex was paralyzed with 5% homatropine, and the nictitating membrane was retracted with 10% phenylephrine. The cornea was protected with a zero-power contact lens containing an artificial pupil with a 2-mm diameter.

Cortical recordings were made with resin-coated tungsten microelectrodes (0.5–1.0 MΩ or 7–10 MΩ; A-M Systems). The RFs of the recorded neurons were located in the central 30° of the visual field. The raw voltage of the spike signal was digitized at a 10-kHz sampling rate with a data acquisition board (National Instruments) running under LabVIEW (National Instruments). Single units were isolated off-line by setting a voltage threshold. The visual test stimuli were back-projected on a tangent screen with a DLP projector (120-Hz refresh rate; AskProxima M1, InFocus). The distance between the screen and the animal was 60 cm. The visual stimuli were created with Psychophysics Toolbox and SimpleGL functions. We also recorded cortical activity from two normally reared, awake behaving juvenile ferrets at PND43 and PND47, while they watched the flickering- and drifting-spots movies, using the multielectrodes as described previously (Ohshiro and Weliky 2006).

Sinusoidal grating stimuli (100% contrast, mean luminance: 50 cd/m^2) with spatial frequencies of 4.0, 6.8, 9.6, or 12.4°/cycle, drifting at 2 Hz, were used to measure the orientation/direction selectivity of cortical neurons. Gratings were presented at 18 different directions (20° apart), ranging from 0° to 340°. For each

direction, gratings were shown for 4 s, followed by 4 s of blank gray screen. After all of the 18 directions were presented, the entire process was repeated a total of four to six times. The mean spike counts recorded during the presentation of gratings (4 s) were used to generate the orientation/direction tuning histograms (Fig. 2*A*). The raw histograms were normalized from 0 to 1, aligned with their largest spike bin (Bin_{Max}) at the center, and averaged to obtain the averaged histogram in Fig. 2*B*. The orientation selectivity index (OSI) was calculated as described previously (Weliky and Katz 1997). Briefly, with Fourier analysis, the amplitudes of the 0th and the 2nd harmonic component of the histogram were computed. The OSI was obtained by dividing the latter by the former. The direction selectivity index (DSI) was calculated from the histogram as follows:

$$DSI = (R_{Pref} - R_{Null})/(R_{Pref} + R_{Null}) \quad (1)$$

where R_{Pref} is the spike count in the Bin_{Max} plus the two flanking bins of the histogram; R_{Null} is the spike count in the bin at 180° away from the direction corresponding to Bin_{Max} plus the spike counts in the two flanking bins. The tuning curve half-bandwidth at $1/\sqrt{2}$ height, simply referred to as the bandwidth of the neuron, was computed as described previously (Ringach et al. 2002b). The 95% confidence interval of the mean (Fig. 3) was obtained by Student's *t*-test.

Simple-cell RFs were mapped with the reverse correlation technique using the m-sequence (Reid et al. 1997; Usrey et al. 2003). Three different m-sequences of length 2^{13}-1 (order $n = 13$) were generated with the feedback taps p = 28, 39, and 53. Two-dimensional white noise stimuli consisting of a 16 × 16 grid of pixels, either black or white, were created from these m-sequences. An inverted repeat counterpart of each m-sequence was also created (Benardete and Victor 1994). The size of individual pixels ranged between 0.75° and 2.0° of visual angle on a side. The stimulus was updated every 50 ms. Presentation of the entire sequence took ~7 min. Typically, two sets of the inverted repeat pairs were presented (total ~28 min) for a RF map. The raw RF map obtained was smoothed by a Gaussian filter and is displayed in Fig. 4, *A* and *B*. The raw RF map was further fit with a Gabor function:

$$G(x', y') = A \cdot \exp\left[-(x'/\sqrt{2}\sigma_{x'})^2 - (y'/\sqrt{2}\sigma_{y'})^2\right] \cdot \cos(2\pi \cdot f \cdot x' + \phi) \quad (2)$$

$$\begin{pmatrix} x' \\ y' \end{pmatrix} = \begin{pmatrix} \cos\theta & \sin\theta \\ -\sin\theta & \cos\theta \end{pmatrix} \begin{pmatrix} x - x_0 \\ y - y_0 \end{pmatrix} \quad (3)$$

where (x_0 y_0) corresponds to the center of the fitted Gaussian envelope, f represents the spatial frequency of the sinusoidal grating in cycles/pixel, and θ is equal to the angle between the y-axis of the original map coordinate and the longitudinal axis of the fitted simple-cell RF parallel to the alternating ON/OFF subfields. The length-to-width ratio of the dominant subfield (Fig. 4*C*) was computed from the fitted Gabor function, as described previously (Usrey et al. 2003). $n_x = f \cdot \sigma_x$ and $n_y = f \cdot \sigma_y$ were also computed based on the fit parameters and are projected on the scatterplot shown in Fig. 4*D* (Ringach 2002).

Simulation of simple-cell RF development. Grayscale images of natural scenes, short bars, and sparse spots were first band-pass filtered with a model LGN neuron (Fig. 5*A*) (Ohshiro and Weliky 2006). The spatial RF of the LGN neuron was modeled as a difference of Gaussian functions:

(4)

$$K_c \cdot \left(\frac{1}{2\pi\sigma_c}\right) \cdot \exp\left[-\frac{(x^2+y^2)}{2\sigma_c^2}\right] - K_s \cdot \left(\frac{1}{2\pi\sigma_s}\right) \cdot \exp\left[-\frac{(x^2+y^2)}{2\sigma_s^2}\right]$$

where $K_c = 1.0$, $K_s = 0.8$, $\sigma_c = 1.6$ (pixel), and $\sigma_s = 4.8$ (pixel). K_s takes a value <1.0 to model the weak surround of the LGN neurons in young ferrets (see Supplemental Fig. S2). In this modeling study, we assumed that a 16 × 16 pixel image patch corresponds to a 10° × 10° (visual angle) area. The model LGN neuron would respond most to a sinusoidal grating stimulus at the spatial frequency of ∼10°/cycle, which is similar to those values obtained from typical X-type LGN neurons in young ferrets (see Supplemental Fig. S2). The sparse spots visual stimuli used in the model simulation contained black or white spot images with a diameter of 2.5° of visual angle. The diameter of the spot (about one-fourth of the model cortical RFs) and its density were chosen such that those values roughly matched the parameters for the spot stimuli used in the actual movie training. The bar stimuli contained black or white full-field bars with widths of 2.5° of visual angle.

The initial cortical RFs have "halos" of ON/OFF-responsive area (Fig. 5, *B–E*) to model an immature RF with weak orientation selectivity. An activity-independent mechanism, such as the haphazard retinal input sampling mechanism, could produce such biased initial RFs before the onset of visual experience (Ringach 2004). These RFs were created by first simulating the random sampling pattern of the ON/OFF mosaic (Ringach 2004) and then blurring the pattern with a Gaussian filter.

For the correlation-based model simulation, we followed the details described in previous articles (Miller 1994; Ohshiro and Weliky 2006). The correlation functions of the model LGN neurons ($C^{ON,ON} = C^{OFF,OFF}$; $C^{ON,OFF} = -0.5C^{ON,ON}$) were obtained by computing the two-dimensional autocorrelation functions of the filtered visual images. A two-dimensional Gaussian function with its σ equal to 3.0 (pixels) was used for the intracortical interaction function. The diameter of the model cortical neuron (i.e., the diameter of the arbor function) was set at 11 pixels (∼7° of visual angle), which was chosen to be similar to those of the simple cells in the young ferret's visual cortex (Fig. 4). The subtractive normalization of synaptic weights (Miller 1994) and the split normalization of synaptic weights (Ohshiro and Weliky 2006) were performed at every update of the weights. The raw RFs were further smoothened with a two-dimensional Gaussian filter and were used for the Gabor function fit analysis (Fig. 6).

For the Bienenstock, Cooper, and Munro (BCM) neuron model, we followed the details described in previous articles (Bienenstock et al. 1982; Blais et al. 1998; Law and Cooper 1994; Lee et al. 2000). The memory constant of the BCM neuron, τ, was set at 300. The maximum and minimum values of the sigmoidal-shape cortical activation function were set at +10 and −1, respectively. Circular patches of 16-pixel diameter, sampled from the filtered images, served as inputs to the model cortical neuron.

For the sparse-coding model, we followed the details described in previous articles (Olshausen 2002; Olshausen and Field 1996). We performed a virtual reverse-correlation mapping with single-pixel visual stimuli and obtained the "receptive fields," which are shown in Fig. 5*B*.

RESULTS

Dark rearing of visually inexperienced, juvenile ferrets was started at PND26–28, which is approximately 1 wk before natural eye opening. Once the ferrets' eyelids naturally opened, visual training was started. The ferret pups were restrained in chambers in a darkroom (Fig. 1*A*), and one of the following movies was presented to each group of ferrets: *1*) a drifting-bars movie (Fig. 1*B*, *left*), *2*) a flickering-spots movie (Fig. 1*B*, *middle*), or *3*) a drifting-spots movie (Fig. 1*B*, *right*). The experimenter wore binocular night vision goggles and set up the training sessions in complete darkness. Daily training sessions were performed for up to 4 h a day and lasted for 4–7 wk until the critical period of visual cortical plasticity had

ended (Issa et al. 1999). Three control groups were also included in the experiment: *1*) a normally reared control group, *2*) a restraint control group, and *3*) a dark-reared control group. The restrained control group viewed ordinary laboratory scenes while restrained in the chamber and was included to see whether physical restraint in the chamber had any effect on the development of cortical selectivity (see METHODS for detailed visual training procedures).

Terminal electrophysiological experiments were conducted to examine the visual cortical selectivity of these trained animals. We examined three ferrets from the normally reared group ($n = 30$ neurons), three ferrets from the restraint group ($n = 51$ neurons), three ferrets from the drifting-bars movie group ($n = 45$ neurons), seven ferrets from the flickering-spots movie group ($n = 91$ neurons), seven ferrets from the drifting-spots movie group (93 neurons), and three ferrets from the dark-reared group ($n = 48$ neurons). Orientation/direction tuning histograms were created for each neuron by presenting drifting grating stimuli (Fig. 2*A*). The tuning histograms of all groups, except for the dark-reared group, exhibited clearly appreciable peaks, indicating that orientation selectivity was substantially developed in all visually experienced groups. To visualize the overall trend of the tuning histograms, the tuning histograms were normalized from 0 to 1 and averaged for each group (Fig. 2*B*). These averaged histograms could be readily distinguished by the height of the troughs flanking the central peak. The dark-reared group showed the highest trough, whereas all averaged histograms from visually experienced groups showed substantially lower troughs. Because the magnitude of response to the preferred orientation (peak) relative to responses at orthogonal orientations (trough) reflects the neuron's orientation selectivity, the highest trough of the dark-reared group suggests poorly developed orientation selectivity in this group. The poor orientation selectivity of the dark-reared animals is consistent with the previous finding that dark rearing arrests the maturation of orientation selectivity (White et al. 2001). Notably, the averaged histograms of all the visually experienced groups were almost undistinguishable, except for the drifting-spots movie group, whose histogram showed a significantly higher trough than other visually experienced groups.

To summarize the effects of visual training, we conducted population analyses for individual neurons (Fig. 3). An OSI, ranging from 0.0 to 1.0 (poor to strong selectivity, respectively; see METHODS), was computed for each raw tuning histogram, and the group mean and its 95% confidence interval are plotted in Fig. 3*A*. The differences in these mean OSI values are statistically significant ($P \ll 0.001$, 1-way ANOVA). Consistent with the conclusion from Fig. 2*B*, a post hoc multiple-comparison test indicated that the mean OSI of the dark-reared group is significantly lower than that of any other group (Scheffé's test, $\alpha = 0.05$). The same statistical test also revealed that the mean OSI of the drifting-spots movie group is marginally lower than that of the flickering-spots movie group. The bandwidth of the tuning histogram, another measure of orientation selectivity (Ringach et al. 2002b), revealed the same trend as in the OSI (Fig. 3*B*): groups with lower OSI values tended to show broader bandwidths. These analyses confirm that orientation selectivity was substantially developed in all visually experienced groups. We can draw several conclusions on the effects of the visual training. The strong orientation selectivity demonstrated in the restraint group, which was comparable to that of the normally reared group, indicates that physical restraint in the chamber had little, if any, effect on orientation selectivity development. The fairly good orientation selectivity in the drifting-bars movie group suggests that the visual experience of the elongated bars was sufficient for the development of orientation selectivity, as expected. Most importantly, the cortical neurons of ferrets in both the flickering- and drifting-spots movie groups exhibited substantially developed orientation selectivity, suggesting that contour visual experience was not absolutely required for orientation selectivity development.

We also examined the direction selectivity of cortical neurons. A DSI, ranging from 0.0 to 1.0 (poor to strong selectivity, respectively; see METHODS), was computed for each raw tuning histogram, and the group mean and its 95% confidence interval are plotted in Fig. 3*C*. The distribution of the mean DSI shows a trend similar to that of OSI: the dark-reared group showed lower direction selectivity than all other visually experienced groups. Although the difference in mean DSI values was not statistically significant,

the finding that the normally reared group had a higher mean DSI than all other visually experienced groups might suggest that physical restraint in the chamber impeded full development of direction selectivity. Interestingly, the flickering-spots movie group exhibited substantially developed direction selectivity, although the movie stimulus contained no apparent motion energy. The nonrestrained eye movement during the visual training might contribute to this direction selectivity development (see DISCUSSION).

To provide further evidence of the development of orientation selectivity in the absence of elongated lines, a subset of the visual cortical cells in the drifting- and flickering-spots movie-conditioned ferrets (9 and 11 cells from the flickering- and drifting-spots groups, respectively) were examined for their spatial RF structure (Fig. 4). As in the normally reared ferrets (Usrey et al. 2003), cells with authentic simple-cell RFs consisting of two or three alternating ON/OFF subfields were found in the visual cortices of both the flickering- and drifting-spots stimulus-conditioned ferrets (Fig. 4, *A* and *B*). The polar plot of the orientation tuning curve depicted below the individual spatial RF map demonstrates that the preferred orientation predicted from the tuning curve largely matched the preferred orientation predicted from the RF structure. Thus these cells were functional in terms of detecting oriented lines/edges and are presumed to underlie the substantial orientation selectivity demonstrated in these ferrets. The spatial RF of these neurons was further fit with a Gabor function (see METHODS), and the length-to-width aspect ratio for a simple-cell RF subfield (Usrey et al. 2003) was computed. The aspect ratios among our samples ranged from ~1 to 3, with means of 1.4 and 1.6 for the flickering-spots and drifting-spots movie groups, respectively (Fig. 4*C*). These means were nearly 60% of the reported value for the simple cells of adult ferrets (Usrey et al. 2003), suggesting that the simple-cell subfields in our sample are less elongated. We also computed n_x,n_y, which represent the size of the elliptic Gaussian envelope measured in units of the period of the sinusoidal grating (Ringach 2002). The distribution of (n_x,n_y) in our sample, along with the corresponding distribution in macaque V1 (Ringach 2002), is shown in Fig. 4*D*. The scatterplot shows that the data points of our sample lie in a relatively limited area in the space, in which bloblike RFs and simple-cell RFs with two subfields are predominantly mapped (Ringach 2002).

The LGN neurons of the flickering- and drifting-spots stimuli-conditioned ferrets exhibited well-developed antagonistic surround in their RFs (Supplemental Fig. S2), suggesting that the peripheral visual neurons had also developed functional RFs under these visual stimuli conditions (Akerman et al. 2002; Tavazoie and Reid 2000).

A number of neural network models based on the Hebbian learning mechanism (Hebb 1949; von der Malsburg 1973) have been proposed to account for simple-cell RF development through visual experience. Some of these models are characterized by unique implementations of the Hebbian mechanism, which make the network sensitive to the "higher-order" statistical information of the visual inputs (Bell and Sejnowski 1997; Blais et al. 1998; Hyvärinen et al. 2001; Law and Cooper 1994; Olshausen and Field 1996; van Hateren and Ruderman 1998). Simple-cell RFs arise in these models as a result of the network's learning of the information representing edges/contours. Indeed, two such models account for development of simple-cell RFs with naturalistic image inputs (Fig. 5, *B1* and *C1*) and elongated-bar image inputs (Fig. 5, *B2* and *C2*). However, these models produce center-surround-type RFs when given sparse-spots image inputs (Fig. 5, *B3* and *C3*). This result indicates that these models are unable to account for our experimental finding (Fig. 4). We next examined a different class of model involving a much simpler Hebbian learning rule. The model utilizes a correlation-based rule (Miller 1994) by which the synaptic efficacy between a presynaptic input and the postsynaptic neuron strengthens or weakens in simple proportion to the correlation of their activities. The original correlation-based model includes a subtractive normalization mechanism in which the total synaptic efficacy from the ON- or OFF-center LGN inputs is conserved during development (Miller 1994). This model predicts RFs with multiple ON/OFF subfields for all three types of visual input (Fig. 5, *D1–D3*). However, a substantial proportion of the predicted RFs includes bloblike RFs with only a single (i.e., "ON" or "OFF") subfield (Fig. 6*A*). Next, we examined the

same model with a split constraint—a different synaptic weight conservation mechanism in which the total synaptic efficacy is conserved separately for the ON- or OFF-center LGN inputs (Ohshiro and Weliky 2006). The model also predicts RFs with multiple ON/OFF subfields for all three types of visual input, and most of the RFs show segregated ON/OFF subfields (Fig. 5, *E1–E3*, and Fig. 6*B*). We further fitted the RFs predicted by the two models with a Gabor function, and the distribution of (n_x,n_y) is displayed in Fig. 6, *C* and *D*, along with the real simple-cell data from the flickering- and drifting-spots movie-conditioned animals. The center of the distribution in the model with the subtractive normalization (Fig. 6*C*) is located near $(n_x,n_y) \approx (0.1,0.1)$, reflecting the fact that the model predicts predominantly bloblike RFs (Fig. 6*A*). This model accounts for a small portion of the real simple-cell data, which corresponds to bloblike RFs or RFs with two alternating subfields. On the other hand, the distribution in the model with the split constraint (Fig. 6*D*) is concentrated near $(n_x,n_y) \approx (0.2,0.2)$ and extended to an area with higher values, reflecting the fact that the model predicts RFs with multiple segregated ON/OFF subfields, including those with three lobes, as seen in Fig. 4*B*. Therefore, the model with the split constraint accounts better for the distribution in the data from real simple-cell RFs. These simulation results suggest that a Hebbian learning mechanism as simple as the correlation-based rule, and possibly supplemented with the split constraint mechanism, might underlie cortical orientation selectivity development after the onset of visual experience.

DISCUSSION

Neurons with rudimentary orientation selectivity and simple-cell RFs are already present in the visually inexperienced cortex, but visual experience is necessary for full maturation of orientation selectivity (Braastad and Heggelund 1985; Chapman et al. 1996; Crair et al. 1998; White et al. 2001). White et al. (2001) clearly demonstrated that patterned visual stimulation is critical for cortical selectivity development. In the present study, we demonstrate, for the first time, that visual stimulation with dynamic sparse spots is sufficient for orientation selectivity development. The finding may not seem to correspond with the notion that the primary visual cortex develops the edge detector property (i.e., cortical orientation selectivity) through visual experience of edges/contours during early life. Supporting this view, a number of neural network models have proposed that the simple-cell RF is the result of the network's learning of edges/contours from visual inputs (Bell and Sejnowski 1997; Blais et al. 1998; Law and Cooper 1994; Olshausen and Field 1996; van Hateren and Ruderman 1998). However, our experimental finding that contour visual experience is not necessary for orientation selectivity development is inconsistent with this view. In contrast to these models, Linsker's model for simple-cell RF development (Linsker 1986; MacKay and Miller 1990) and Miller's correlation-based model (Miller 1994), which is a simplified version of Linsker's model (Miller 1990), do not explicitly require edges/contours in the visual inputs. Critically, the correlation-based model with synaptic weight constraints can produce simple-cell RFs with sparse, small spot stimuli (Figs. 5 and 6), consistent with our experimental finding (Fig. 4). Putting different constraints on synaptic weight dynamics might drastically alter the resulting RFs (Goodhill and Barrow 1994; Miller 1996; Miller and MacKay 1994). We showed that the correlation-based model with the split constraint mechanism accounts better for our experimental results (Fig. 6). The split constraint mechanism helps simple-cell RFs with multiple ON/OFF subfields to emerge stably for a broad range of model parameters (not shown). The split constraint mechanism was initially proposed to reconcile a prediction of the correlation-based model with experimental results (Ohshiro and Weliky 2006) and is still only hypothetical. Notably, when the ratio of the diameter of the model LGN neuron to the cortical neuron is assumed to be smaller than a certain value, both synaptic normalization mechanisms lead to identical simple-cell RFs with multiple ON/OFF subfields (not shown). Therefore, the difference in model prediction shown in this study seems to originate from the particular set of model parameters used (see METHODS), which are nonetheless based on the experimentally measured values. Validation of the synaptic normalization mechanism awaits future study investigating the mechanism at the molecular level.

Miller (1994) showed that for simple-cell RFs to emerge in the cortex, his correlation-based model requires a Mexican hat-shaped pattern of correlated activity to be present among LGN neurons (Miller 1992, 1994). Previously, we performed multielectrode recordings from LGN neurons in awake behaving ferrets (Ohshiro and Weliky 2006) and found a Mexican hat-shaped pattern of correlated activity in the LGN of normal control animals viewing a dynamic white noise stimulus—a stimulus similar to the flickering-spots stimulus used in this study. This observation suggested that if the correlation-based model were correct, continuous visual stimulation with a white noise (or flickering spots) stimulus should be sufficient for simple cells to emerge in the visual cortex. The present experiment using the dynamic-spots stimulus was motivated by this idea. The center-surround structure of the RFs of LGN neurons is critical for the Mexican hat-shaped pattern of correlated activity to be present in LGN neurons (Miller 1994; Ohshiro and Weliky 2006). The LGN neurons of the flickering- and drifting-spots stimuli-conditioned ferrets exhibited well-developed antagonistic surround (see Supplemental Fig. S2). It can therefore be assumed that a Mexican hat-shaped pattern of correlated activity was present among the LGN neurons in these animals during visual stimulation.

In marked contrast to orientation selectivity, which develops under extremely poor visual conditions (Cremieux et al. 1987; Olson and Pettigrew 1974), the emergence of cortical direction selectivity has been shown to be critically dependent on visually experiencing motion (Cynader and Chernenko 1976; Humphrey and Saul 1998; Humphrey et al. 1998; Li et al. 2006). However, a more detailed two-photon calcium imaging study revealed that some neurons in the visually naive cortex exhibit a weak directional response bias, and there is already a weak coherent spatial organization of direction preferences in the visually naive cortex (Li et al. 2008). Visually experiencing motion seems to amplify the early bias and to help the emergence of a spatially coherent map for the direction-selective response. A similar account is possible for the development of orientation selectivity. Rudimentary simple-cell RFs may appear in the immature cortex through endogenous spontaneous neural activity (Linsker 1986; Miller 1994) or the haphazard wiring mechanism of retinal inputs (Ringach 2004). After the onset of visual experience, competition and collaboration between the ON-/OFF-centered LGN afferents, mediated through the Hebbian synaptic plasticity mechanism and the synaptic weight constraint mechanism (Goodhill and Barrow 1994; Miller 1994, 1996; Miller and MacKay 1994), lead to the segregated ON/OFF subfields seen in mature simple-cell RFs. Further interaction between cortical neurons through lateral connections (Miller 1994) allows nearby neurons to correlate their activity, and this correlated activity guides the emergence of a smooth, spatially coherent map of selectivity over the cortex. Our experimental result argues against the idea that contour visual experience creates the orientation selectivity de novo. Rather, we suggest that visual experience amplifies the early fluctuation in functional architecture responsible for the weak orientation and direction selectivity bias in the immature cortex and consolidates the selectivity maps built on the early biased functional architecture. Please also note that Miyashita and Tanaka's model—a model related to the correlation-based model (Miyashita et al. 1997)—allows spontaneous emergence of direction selectivity without visually experiencing motion.

Ferrets have contour vision through closed eyelids as early as PND21 (Akerman et al. 2004; Krug et al. 2001), about a week before the dark rearing began in this study. Thus the visually trained ferrets used in this study possibly had experienced contour vision prior to the beginning of the experiment. The early visual experience through closed eyelids is shown to be essential for retinogeniculate pathway development (Akerman et al. 2002) and might also contribute to establishment of the early functional architecture for the weak orientation and direction selectivity before eye opening. The rudimentary cortical selectivity eventually dies out in the absence of the visual experience, as shown in the dark-reared group (Figs. 2 and 3; Crair et al. 1998; White et al. 2001).

Interestingly, we observed that the neurons of the flickering-spots movie-conditioned animals showed substantial development of direction selectivity, even though the training movie stimulus contained no apparent motion energy (Fig. 3*C*). The early bias in direction selectivity present in the immature cortex

might have survived after the continuous visual stimulation during the flickering-spots movie. Alternatively, the unrestrained eye movement during the movie presentation might have created apparent motion of the spot's image, which might be sufficient for direction selectivity development. One could also argue that an animal's rapid eye movement while viewing the flickering-spots stimulus generates oriented "motion streaks" (Geisler 1999) that would produce visual activation similar to that with oriented stimuli (Jancke 2000), particularly because the temporal integration time of the immature visual neurons is long (Cai et al. 1997). We adopted a rather moderate rate (~3 Hz) as the flickering frequency for the spot stimuli to have robust neural responses in the LGN (not shown). As we did not control eye movement or estimate its magnitude during visual training, we cannot exclude the possible effect of eye movement on cortical selectivity development in our experimental animals.

Another interesting observation is that the drifting-spots movie stimulus was less effective in promoting cortical orientation selectivity then the flickering-spots movie stimulus (Fig. 2). Considering that cortical cells respond to the spatiotemporal energy of visual inputs (Basole et al. 2003), the drifting-spots stimulus should excite the cortical cells less effectively because of the noncoherent motion of the spots. Indeed, the visual cortical neurons of the awake juvenile ferrets at PND43 and PND47 responded less to the drifting-spots stimulus than to the flickering-spots stimulus. The mean firing rates (spikes/s) were as follows: flickering-spots movie = 6.2; drifting-spots movie = 5.4 (total $n = 39$ neurons, $P = 0.053$, paired t-test). The maximum spike rates (spikes/50-ms bin) were as follows: flickering-spots movie = 7.2; drifting-spots movie = 6.2 ($P = 0.003$). We assume that the continuous, but weaker, activation of cortical cells in response to the drifting-spots stimulus prevented the full development of cortical selectivity in the drifting-spots stimulus-conditioned animals. Because we found functional simple cells in these animals (Fig. 3*B*), we speculate that the intracortical inhibition essential for sharpening orientation selectivity (Blakemore and Tobin 1972; Hata et al. 1988; Ringach et al. 2002a, 2003; Sato et al. 1996) was impaired in the visual cortices of these animals. The higher troughs seen in the averaged tuning histogram of the flickering-spots group is consistent with this speculation. More sophisticated RF mapping techniques (Ringach et al. 1997a, 1997b) will be useful to clarify the issue in future studies.

Because of the insufficient number of trained animals, we could not afford to examine other prominent features of the visual cortex, including the spatial-phase relationship of ON/OFF subfields between neighboring simple cells (DeAngelis et al. 1999; Jin et al. 2008, 2011) and the segregation of the ON and OFF afferents in the cortex (Jin et al. 2008; Zahs and Stryker 1988). The correlation-based model has a specific prediction about these two features (Miller 1994). Importantly, the correlation-based model with the split constraint and the original model with the subtractive normalization predict a gradual shift in the spatial phase of ON/OFF subfields in neighboring neurons (Fig. 6, *A* and *B*), which is the direct consequence of the segregation of the ON and OFF afferents in the cortex in these models (Supplemental Fig. S3). These features, however, depend primarily on the shape of the intracortical interaction function (Miller 1994), which is assumed in these models to be fixed (a broad Gaussian-shaped function) during development. It will be interesting to directly measure the function in the developing cortex and to examine a model including the measured function to compare to experimental data.

GRANTS

This work was supported by a National Eye Institute grant. T. Ohshiro acknowledges a support from Japan Society for the Promotion of Science.

DISCLOSURES

No conflicts of interest, financial or otherwise, are declared by the author(s).

Supplementary Material

Supplemental Figures:

ACKNOWLEDGMENTS

We thank Kenneth Miller, David Fitzpatrick, Ye Li, Leonard White, and Gregory DeAngelis for helpful comments on the manuscript. We also thank W. Martin Usrey, Robert Emerson, Akiyuki Anzai, and Takahisa Sanada for technical advice on the cortical recording. We especially thank the University of Rochester Committee on Animal Resources for helping us to establish the animal training protocol and volunteer graduate students for helping us with the animal training.

Footnotes

[1]Supplemental Material for this article is available online at the Journal website.

REFERENCES

Akerman CJ, Grubb MS, Thompson ID. Spatial and temporal properties of visual responses in the thalamus of the developing ferret. J Neurosci 24: 170–182, 2004 [PubMed: 14715950]

Akerman CJ, Smyth D, Thompson ID. Visual experience before eye-opening and the development of the retinogeniculate pathway. Neuron 36: 869–879, 2002 [PubMed: 12467590]

Basole A, White LE, Fitzpatrick D. Mapping multiple features in the population response of visual cortex. Nature 423: 986–990, 2003 [PubMed: 12827202]

Bell AJ, Sejnowski TJ. The “independent components” of natural scenes are edge filters. Vision Res 37: 3327–3338, 1997 [PMCID: PMC2882863] [PubMed: 9425547]

Benardete EA, Victor JD. An extension of the m-sequence technique for the analysis of multi-input nonlinear systems. In: Advanced Methods of Physiological Systems Modeling, edited by Marmarelis VZ, editor. New York: Plenum, 1994, p. 87–110

Bienenstock EL, Cooper LN, Munro PW. Theory for the development of neuron selectivity: orientation specificity and binocular interaction in visual cortex. J Neurosci 2: 32–48, 1982 [PubMed: 7054394]

Blais BS, Intrator N, Shouval HZ, Cooper LN. Receptive field formation in natural scene environments. Comparison of single-cell learning rules. Neural Comput 10: 1797–1813, 1998 [PubMed: 9744898]

Blakemore C, Cooper GF. Development of the brain depends on the visual environment. Nature 228: 477–478, 1970 [PubMed: 5482506]

Blakemore C, Tobin EA. Lateral inhibition between orientation detectors in the cat's visual cortex. Exp Brain Res 15: 439–440, 1972 [PubMed: 5079475]

Blakemore C, Van Sluyters RC. Innate and environmental factors in the development of the kitten's visual cortex. J Physiol 248: 663–716, 1975 [PMCID: PMC1309546] [PubMed: 1151843]

Braastad BO, Heggelund P. Development of spatial receptive-field organization and orientation selectivity in kitten striate cortex. J Neurophysiol 53: 1158–1178, 1985 [PubMed: 3998804]

Brainard DH. The Psychophysics Toolbox. Spat Vis 10: 433–436, 1997 [PubMed: 9176952]

Cai D, DeAngelis GC, Freeman RD. Spatiotemporal receptive field organization in the lateral geniculate nucleus of cats and kittens. J Neurophysiol 78: 1045–1061, 1997 [PubMed: 9307134]

Chapman B, Stryker MP, Bonhoeffer T. Development of orientation preference maps in ferret primary visual cortex. J Neurosci 16: 6443–6453, 1996 [PMCID: PMC2669086] [PubMed: 8815923]

Chapman B, Zahs KR, Stryker MP. Relation of cortical cell orientation selectivity to alignment of receptive fields of the geniculocortical afferents that arborize within a single orientation column in ferret visual cortex. J Neurosci 11: 1347–1358, 1991 [PubMed: 2027051]

Crair MC, Gillespie DC, Stryker MP. The role of visual experience in the development of columns in cat visual cortex. Science 279: 566–570, 1998 [PMCID: PMC2453000] [PubMed: 9438851]

Cremieux J, Orban GA, Duysens J, Amblard B. Response properties of area 17 neurons in cats reared in stroboscopic illumination. J Neurophysiol 57: 1511–1535, 1987 [PubMed: 3585478]

Cynader M, Chernenko G. Abolition of direction selectivity in the visual cortex of the cat. Science 193: 504–505, 1976 [PubMed: 941025]

DeAngelis GC, Ghose GM, Ohzawa I, Freeman RD. Functional micro-organization of primary visual cortex: receptive field analysis of nearby neurons. J Neurosci 19: 4046–4064, 1999 [PubMed: 10234033]

Fiser J, Chiu C, Weliky M. Small modulation of ongoing cortical dynamics by sensory input during natural vision. Nature 431: 573–578, 2004 [PubMed: 15457262]

Geisler WS. Motion streaks provide a spatial code for motion direction. Nature 400: 65–69, 1999 [PubMed: 10403249]

Goodhill GJ, Barrow HG. The role of weight normalization in competitive learning. Neural Comput 6: 255–269, 1994

Hata Y, Tsumoto T, Sato H, Hagihara K, Tamura H. Inhibition contributes to orientation selectivity in visual cortex of cat. Nature 335: 815–817, 1988 [PubMed: 3185710]

Hebb DO. The Organization of Behavior; a Neuropsychological Theory. New York: Wiley, 1949

Hirsch HV, Spinelli DN. Modification of the distribution of receptive field orientation in cats by selective visual exposure during development. Exp Brain Res 12: 509–527, 1971 [PubMed: 5093727]

Hirsch HV, Spinelli DN. Visual experience modifies distribution of horizontally and vertically oriented receptive fields in cats. Science 168: 869–871, 1970 [PubMed: 5444065]

Hubel DH, Wiesel TN. Receptive fields of cells in striate cortex of very young, visually inexperienced kittens. J Neurophysiol 26: 994–1002, 1963 [PubMed: 14084171]

Hubel DH, Wiesel TN. Receptive fields of single neurones in the cat's striate cortex. J Physiol 148: 574–591, 1959 [PMCID: PMC1363130] [PubMed: 14403679]

Hubel DH, Wiesel TN. Receptive fields, binocular interaction and functional architecture in the cat's visual cortex. J Physiol 160: 106–154, 1962 [PMCID: PMC1359523] [PubMed: 14449617]

Humphrey AL, Saul AB. Strobe rearing reduces direction selectivity in area 17 by altering spatiotemporal receptive-field structure. J Neurophysiol 80: 2991–3004, 1998 [PubMed: 9862901]

Humphrey AL, Saul AB, Feidler JC. Strobe rearing prevents the convergence of inputs with different response timings onto area 17 simple cells. J Neurophysiol 80: 3005–3020, 1998 [PubMed: 9862902]

Hyvärinen A, Karhunen J, Oja E. Independent Component Analysis. New York: Wiley, 2001

Issa NP, Trachtenberg JT, Chapman B, Zahs KR, Stryker MP. The critical period for ocular dominance plasticity in the ferret's visual cortex. J Neurosci 19: 6965–6978, 1999 [PMCID: PMC2413141] [PubMed: 10436053]

Jancke D. Orientation formed by a spot's trajectory: a two-dimensional population approach in primary visual cortex. J Neurosci 20: RC86, 2000 [PubMed: 10875941]

Jin J, Wang Y, Swadlow HA, Alonso JM. Population receptive fields of ON and OFF thalamic inputs to an orientation column in visual cortex. Nat Neurosci 14: 232–238, 2011 [PubMed: 21217765]

Jin JZ, Weng C, Yeh CI, Gordon JA, Ruthazer ES, Stryker MP, Swadlow HA, Alonso JM. On and off domains of geniculate afferents in cat primary visual cortex. Nat Neurosci 11: 88–94, 2008 [PMCID: PMC2556869] [PubMed: 18084287]

Krug K, Akerman CJ, Thompson ID. Responses of neurons in neonatal cortex and thalamus to patterned visual stimulation through the naturally closed lids. J Neurophysiol 85: 1436–1443, 2001 [PubMed: 11287467]

Law CC, Cooper LN. Formation of receptive fields in realistic visual environments according to the Bienenstock, Cooper, and Munro (BCM) theory. Proc Natl Acad Sci USA 91: 7797–7801, 1994 [PMCID: PMC44489] [PubMed: 8052662]

Lee AB, Blais B, Shouval HZ, Cooper LN. Statistics of lateral geniculate nucleus (LGN) activity determine the segregation of ON/OFF subfields for simple cells in visual cortex. Proc Natl Acad Sci USA 97: 12875–12879, 2000 [PMCID: PMC18857] [PubMed: 11070095]

Li Y, Fitzpatrick D, White LE. The development of direction selectivity in ferret visual cortex requires early visual experience. Nat Neurosci 9: 676–681, 2006 [PubMed: 16604068]

Li Y, Van Hooser SD, Mazurek M, White LE, Fitzpatrick D. Experience with moving visual stimuli drives the early development of cortical direction selectivity. Nature 456: 952–956, 2008 [PMCID: PMC2644578] [PubMed: 18946471]

Linsker R. From basic network principles to neural architecture: emergence of orientation-selective cells. Proc Natl Acad Sci USA 83: 8390–8394, 1986 [PMCID: PMC386934] [PubMed: 3464958]

MacKay DJC, Miller KD. Analysis of Linsker's applications of Hebbian rules to linear networks. Network 1: 257–298, 1990

Miller KD. Derivation of Hebbian equations from a nonlinear model. Neural Comput 2: 319–331, 1990

Miller KD. Development of orientation columns via competition between ON- and OFF-center inputs. Neuroreport 3: 73–76, 1992 [PubMed: 1611038]

Miller KD. A model for the development of simple cell receptive fields and the ordered arrangement of orientation columns through activity-dependent competition between ON- and OFF-center inputs. J Neurosci 14: 409–441, 1994 [PubMed: 8283248]

Miller KD. Synaptic economics: competition and cooperation in synaptic plasticity. Neuron 17: 371–374, 1996 [PubMed: 8816700]

Miller KD, MacKay DJC. The role of constraints in Hebbian learning. Neural Comput 6: 100–126, 1994

Miyashita M, Kim DS, Tanaka S. Cortical direction selectivity without directional experience. Neuroreport 8: 1187–1191, 1997 [PubMed: 9175111]

Ohshiro T, Weliky M. Simple fall-off pattern of correlated neural activity in the developing lateral geniculate nucleus. Nat Neurosci 9: 1541–1548, 2006 [PubMed: 17115045]

Olshausen BA. Sparse codes and spikes. In: Probabilistic Models of the Brain: Perception and Neural Function, edited by Rao RPN, Olshausen BA, Lewicki MS, editors. Cambridge, MA: MIT Press, 2002, p. 257–272

Olshausen BA, Field DJ. Emergence of simple-cell receptive field properties by learning a sparse code for natural images. Nature 381: 607–609, 1996 [PubMed: 8637596]

Olson CR, Pettigrew JD. Single units in visual cortex of kittens reared in stroboscopic illumination. Brain Res 70: 189–204, 1974 [PubMed: 4825670]

Pelli DG. The VideoToolbox software for visual psychophysics: transforming numbers into movies. Spat Vis 10: 437–442, 1997 [PubMed: 9176953]

Reid RC, Alonso JM. Specificity of monosynaptic connections from thalamus to visual cortex. Nature 378: 281–284, 1995 [PubMed: 7477347]

Reid RC, Victor JD, Shapley RM. The use of m-sequences in the analysis of visual neurons: linear receptive field properties. Vis Neurosci 14: 1015–1027, 1997 [PubMed: 9447685]

Ringach DL. Haphazard wiring of simple receptive fields and orientation columns in visual cortex. J Neurophysiol 92: 468–476, 2004 [PubMed: 14999045]

Ringach DL. Spatial structure and symmetry of simple-cell receptive fields in macaque primary visual cortex. J Neurophysiol 88: 455–463, 2002 [PubMed: 12091567]

Ringach DL, Bredfeldt CE, Shapley RM, Hawken MJ. Suppression of neural responses to nonoptimal stimuli correlates with tuning selectivity in macaque V1. J Neurophysiol 87: 1018–1027, 2002a [PubMed: 11826065]

Ringach DL, Hawken MJ, Shapley R. Dynamics of orientation tuning in macaque primary visual cortex. Nature 387: 281–284, 1997a [PubMed: 9153392]

Ringach DL, Hawken MJ, Shapley R. Dynamics of orientation tuning in macaque V1: the role of global and tuned suppression. J Neurophysiol 90: 342–352, 2003 [PubMed: 12611936]

Ringach DL, Sapiro G, Shapley R. A subspace reverse-correlation technique for the study of visual neurons. Vision Res 37: 2455–2464, 1997b [PubMed: 9381680]

Ringach DL, Shapley RM, Hawken MJ. Orientation selectivity in macaque V1: diversity and laminar dependence. J Neurosci 22: 5639–5651, 2002b [PubMed: 12097515]

Sato H, Katsuyama N, Tamura H, Hata Y, Tsumoto T. Mechanisms underlying orientation selectivity of neurons in the primary visual cortex of the macaque. J Physiol 494: 757–771, 1996 [PMCID: PMC1160675] [PubMed: 8865072]

Sherk H, Stryker MP. Quantitative study of cortical orientation selectivity in visually inexperienced kitten. J Neurophysiol 39: 63–70, 1976 [PubMed: 1249604]

Smyth D, Willmore B, Baker GE, Thompson ID, Tolhurst DJ. The receptive-field organization of simple cells in primary visual cortex of ferrets under natural scene stimulation. J Neurosci 23: 4746–4759, 2003 [PubMed: 12805314]

Stryker MP, Sherk H, Leventhal AG, Hirsch HV. Physiological consequences for the cat's visual cortex of effectively restricting early visual experience with oriented contours. J Neurophysiol 41: 896–909, 1978 [PubMed: 681993]

Tanaka K. Cross-correlation analysis of geniculostriate neuronal relationships in cats. J Neurophysiol 49: 1303–1318, 1983 [PubMed: 6875624]

Tanaka S, Ribot J, Imamura K, Tani T. Orientation-restricted continuous visual exposure induces marked reorganization of orientation maps in early life. Neuroimage 30: 462–477, 2006 [PubMed: 16275019]

Tavazoie SF, Reid RC. Diverse receptive fields in the lateral geniculate nucleus during thalamocortical development. Nat Neurosci 3: 608–616, 2000 [PubMed: 10816318]

Usrey WM, Sceniak MP, Chapman B. Receptive fields and response properties of neurons in layer 4 of ferret visual cortex. J Neurophysiol 89: 1003–1015, 2003 [PMCID: PMC2633106] [PubMed: 12574476]

van Hateren JH, Ruderman DL. Independent component analysis of natural image sequences yields spatio-temporal filters similar to simple cells in primary visual cortex. Proc Biol Sci 265: 2315–2320, 1998 [PMCID: PMC1689525] [PubMed: 9881476]

von der Malsburg C. Self-organization of orientation sensitive cells in the striate cortex. Kybernetik 14: 85–100, 1973 [PubMed: 4786750]

Weliky M, Katz LC. Disruption of orientation tuning in visual cortex by artificially correlated neuronal activity. Nature 386: 680–685, 1997 [PubMed: 9109486]

White LE, Coppola DM, Fitzpatrick D. The contribution of sensory experience to the maturation of orientation selectivity in ferret visual cortex. Nature 411: 1049–1052, 2001 [PubMed: 11429605]

Zahs KR, Stryker MP. Segregation of ON and OFF afferents to ferret visual cortex. J Neurophysiol 59: 1410–1429, 1988 [PubMed: 3385467]

Figures and Tables

Fig. 1.

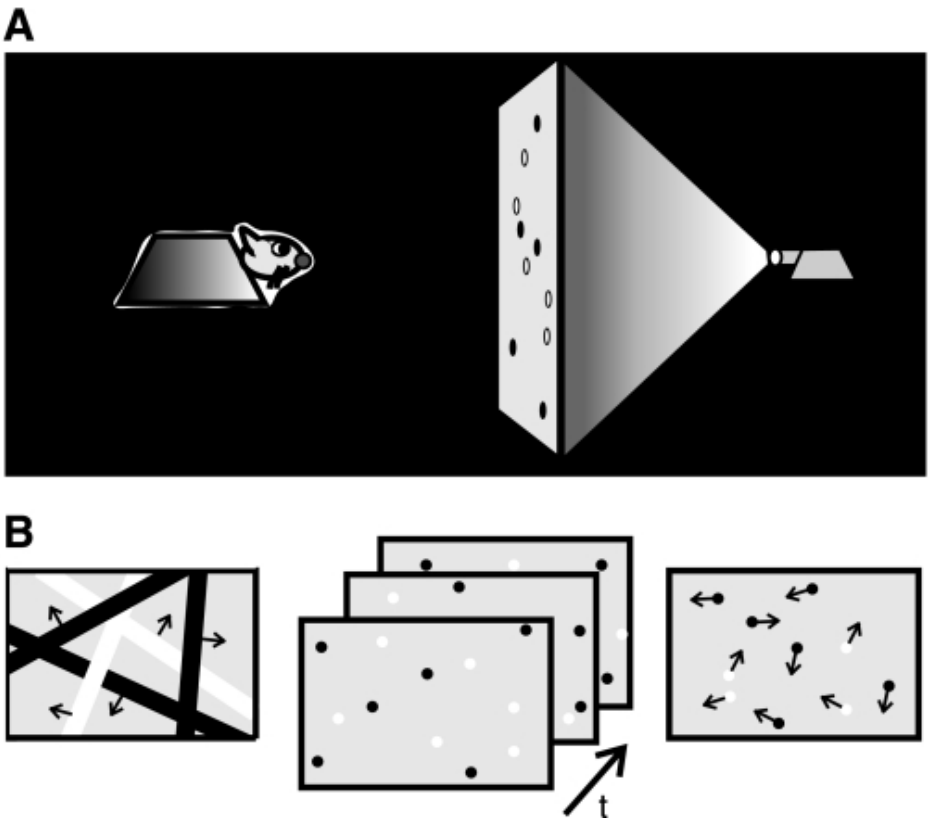

Visual training setup and stimuli. *A*: a ferret pup was restrained in a chamber and viewed a movie back-projected on a large tangential screen (183 cm × 244 cm) placed 60 cm away from the animal. Typically, 2 or 3 ferret pups in restraint chambers were placed side by side and visually trained simultaneously. *B*: the 3 movie stimuli used for the visual training: the drifting-bar movie (*left*), the flickering-spots movie (*middle*), and the drifting-spots movie (*right*). High-contrast dark/bright bars or spots were rendered on the gray background (luminescence 90 cd/m^2). The flickering-spots movie showed high-contrast black or white spots (diameter: 2.5°) appearing at random positions every 375 ms. The density of the spots was 1.1 per 10° × 10° area. The drifting-spots movie showed the same high-contrast black/white spots drifting continuously in random directions at 3.5°/s.

Fig. 2.

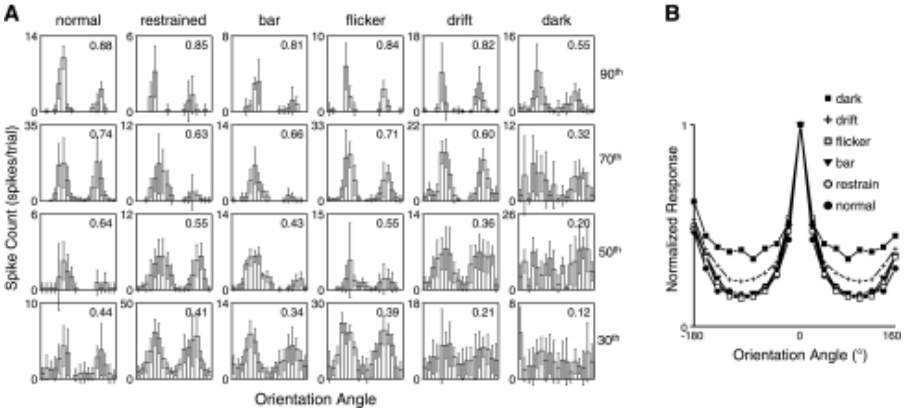

Results of electrophysiological experiments. The cortical orientation selectivity of the experimental animal was assessed by measuring the response to the orientated drifting gratings. *A*: direction/orientation tuning histograms of the visual cortical neurons of the trained ferrets. The orientation selectivity index (OSI) computed from the tuning histogram is shown at *top right* of each histogram. The histograms are sorted by conditioning group (columns) and OSI percentile within the group (rows). Each bar represents the average number of spikes evoked during the stimulus presentation of the gratings drifting in 1 of the 18 directions spanning 0° to 340° (20° apart, *x*-axis). Error bars represent SD. *B*: normalized and averaged tuning histograms from the experimental groups.

Fig. 3.

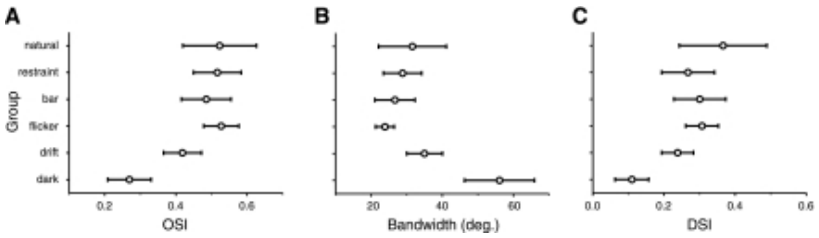

Summary of the visual cortical response properties of the trained animals. Comparison of the group mean for the OSI (*A*), the bandwidth (*B*), and the direction selectivity index (DSI, *C*) of the response-tuning histograms. Error bars represent the 95% confidence interval of the mean.

Fig. 4.

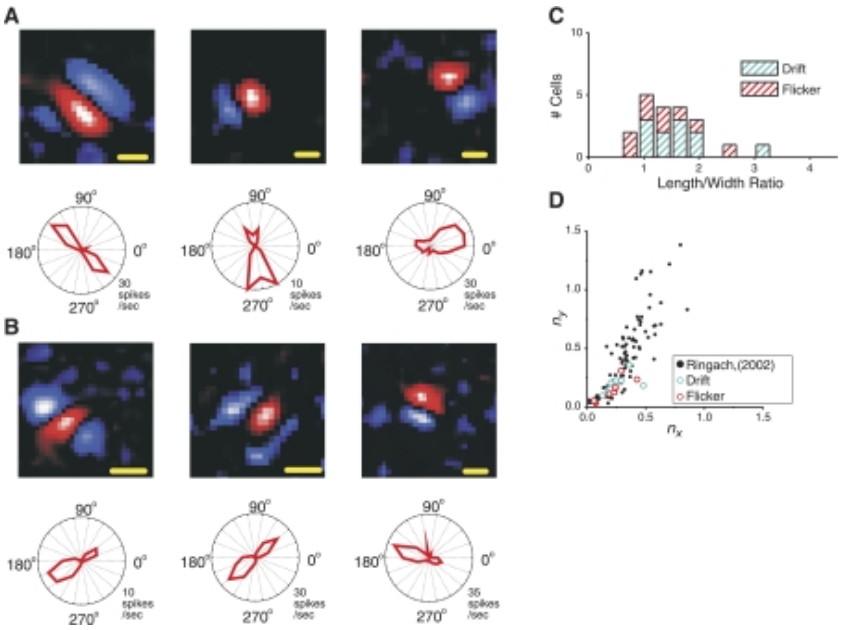

Results of RF mapping experiments. The spatial RF structure of the visual cortical neuron was visualized by the reverse-correlation mapping method. *A*: simple-cell RFs from the flickering-spots movie-conditioned ferrets. *B*: simple-cell RFs from the drifting-spots movie-conditioned ferrets. Red, ON-responsive area; blue, OFF-responsive area. Yellow calibration bar represents 3° of visual angle. The polar plot of the orientation-tuning curve of each example cell is depicted below the individual spatial RF map. The value at 0° in the polar plot represents the mean neural response to the horizontal gratings drifting downward. The orientation of the gratings rotates counterclockwise with increasing angle. *C*: distribution of the length-to-width ratio obtained from the simple cells of the spots movie-conditioned ferrets. *D*: distribution of (n_x,n_y) of the simple-cell RFs from macaque monkeys (black dots), replotted from Ringach (2002), and the corresponding distribution of (n_x,n_y) of the simple cells from spots movie-conditioned ferrets (colored open circles).

Fig. 5.

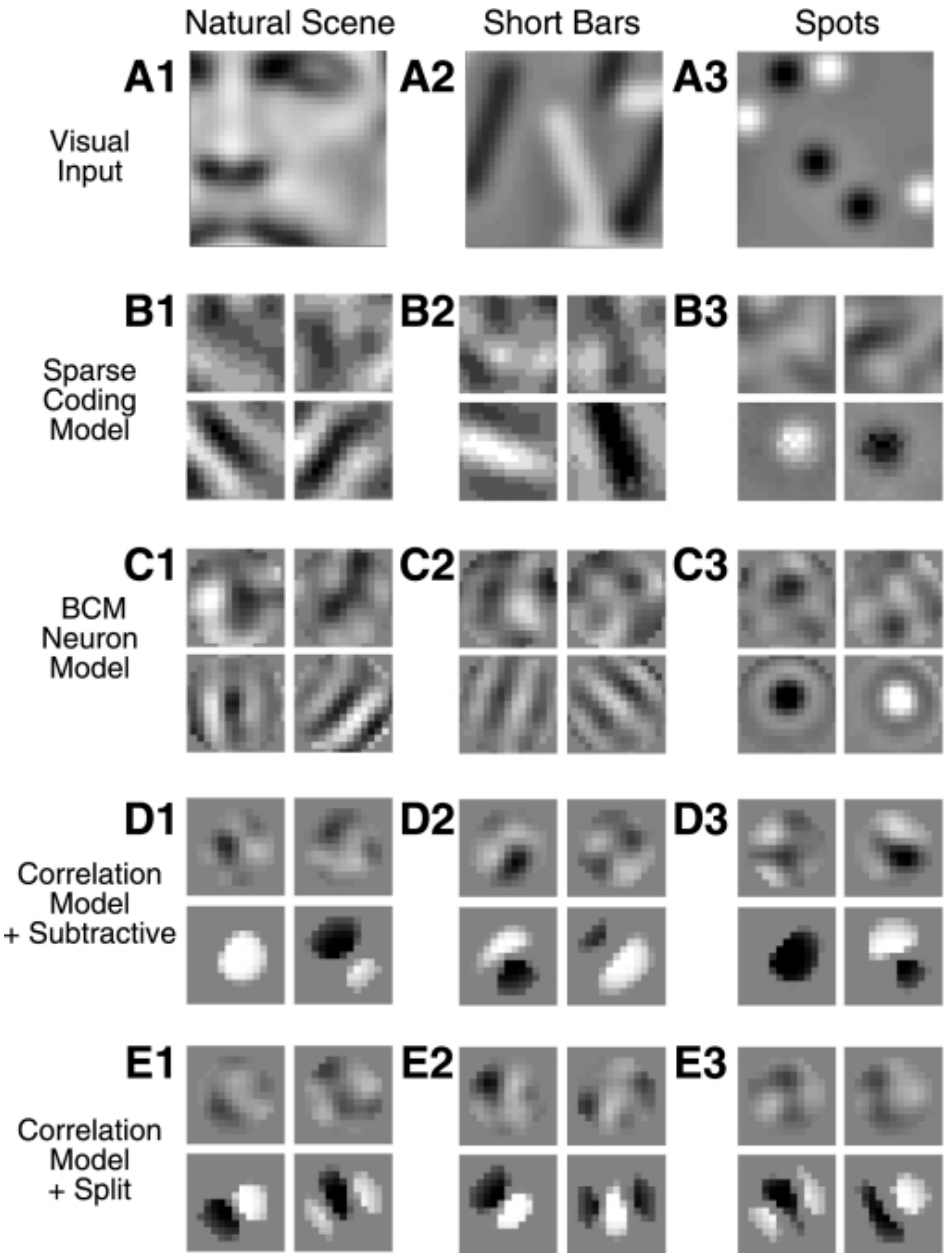

Simulation of spatial RF formation by the sparse-coding model, the Bienenstock, Cooper, and Munro (BCM) neuron model, and the correlation-based model. Each model network was provided with 3 different types of visual inputs: the natural scene images (*A1*), the short bar images (*A2*), and the sparse spots images (*A3*). These visual images were already preprocessed by a realistic LGN spatial filter (see text). The sides of the visual image window are 20° of visual angle. *B1–B3*: simulation results from the sparse-coding model. Each panel corresponds to a window of 10° × 10° of visual angle. Top panels show initial RFs with clumps of the ON/OFF subfields to model the rudimentary simple-cell RF in the immature visual cortex. Bottom 2 panels show the final ON/OFF afferent termination patterns predicted by the model. Bright pixels represent the ON afferent input dominant area, and dark pixels represent the OFF afferent input dominant area. *C1–C3*: simulation results from the BCM neuron model. *D1–D3*: simulation results from the correlation-based model with the subtractive normalization mechanism. *E1–E3*: simulation results from the correlation-based model with the split constraint mechanism.

Fig. 6.

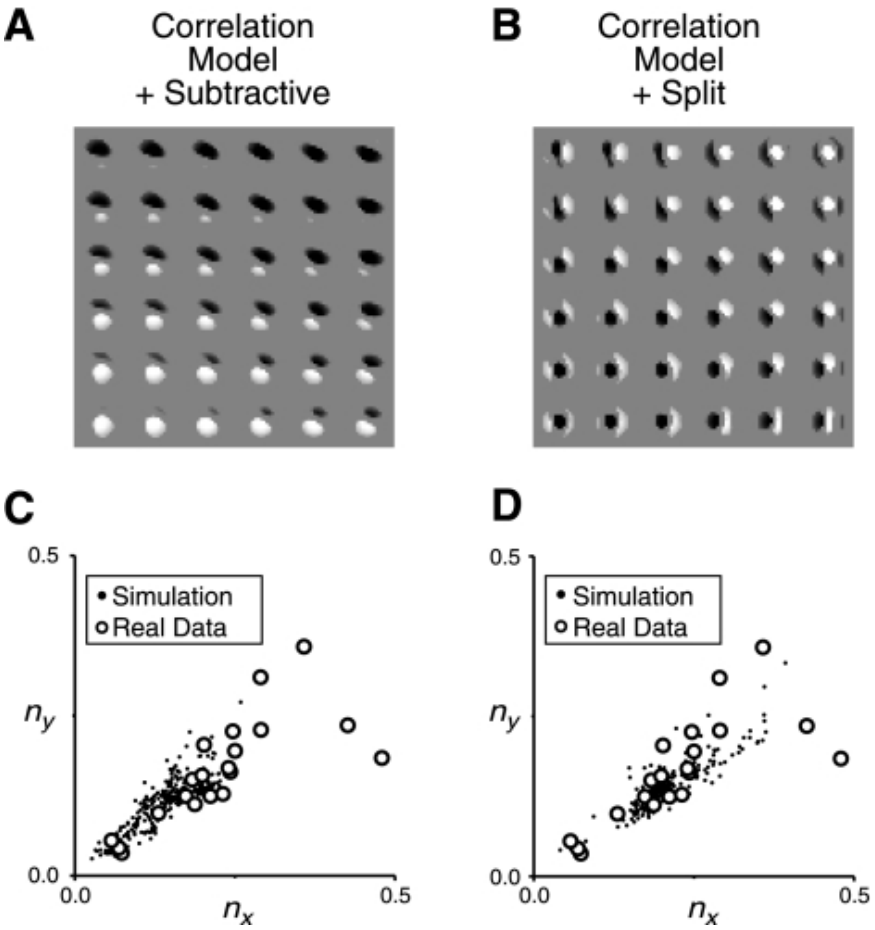

Comparison of the correlation-based models with 2 different synaptic constraint mechanisms. *A*: final RFs of a 6 × 6 patch of cortical cells predicted by the correlation-based model with the subtractive normalization for the sparse spots images. *B*: final RFs predicted by the correlation-based model with the split constraint. *C*: distribution of (n_x,n_y) of the RFs predicted by the model with the subtractive normalization (black dots). Distribution of (n_x,n_y) of the simple-cell RFs from the spots movie-trained animals is simultaneously displayed for comparison (open circles; replotted from Fig. 4*D*). *D*: distribution of (n_x,n_y) predicted by the model with the split constraint mechanism (black dots) and that from the spots movie-trained animals (open circles).